Tumor-Specific Fluorescence-Guided Surgery for Pancreatic Cancer Using Panitumumab-IRDye800CW: A Phase I Dose-Escalation study

Guolan Lu, PhD[1], Nynke S. van den Berg, PhD[1], Brock A. Martin, MD[2], Naoki Nishio, MD[1], Zachary P. Hart[1], Stan van Keulen, MD[1], Shayan Fakurnejad[1], Stefania U. Chirita, MS[1,3], Roan C. Raymundo, BS[1,3], Grace Yi, BS[1,3], Quan Zhou, PhD[1], George A. Fisher, MD[4] [Full Professor], Eben L Rosenthal, MD[1,5] [Full Professor], George A. Poultsides, MD[6,*]

[1]Department of Otolaryngology-Head and Neck Surgery, Stanford University, CA

[2]Department of Pathology, Stanford University, Stanford, CA

[3]Cancer Clinical Trials Office, Stanford University School of Medicine, Stanford, CA

[4]Department of Medical Oncology, Stanford University, Stanford, CA

[5]Stanford Cancer Center, Stanford University, Stanford, CA

[6]Departent of Surgery, Stanford University, Stanford, CA

Abstract

Background—Complete surgical resection remains the primary curative option for pancreatic ductal adenocarcinoma (PDAC) with positive margins in 30%−70% of patients. The present study

*Correspondence to: Dr. George A. Poultsides, Stanford University School of Medicine, 300 Pasteur Drive, H3680, Stanford, CA, USA. gpoultsides@stanford.edu.

aimed to evaluate the use of intraoperative tumor-specific imaging to enhance surgeons' ability to detect visually-occult cancer in real-time.

Methods—In this single-center, open-label, single-arm study, we enrolled patients who had clinically suspicious or biopsy-confirmed PDACs scheduled for curative surgery. Two to five days before surgery, patients were intravenously infused with 100 mg of unlabeled panitumumab followed by 25 mg, 50 mg or 75 mg of the near-infrared (NIR) fluorescently labeled antibody (panitumumab-IRDye800CW). Patients were sequentially enrolled into each dosing cohort. The primary endpoint was to determine the optimal dose of panitumumab-IRDye800CW in identifying PDACs as measured by tumor-to-background ratio (TBR). The TBR was defined as the fluorescence signal of the tumor devided by the fluorescence signal of the surrounding normal tissue. The dose-finding part of this study has been complete. This study is registered with ClinicalTrials.gov, number NCT03384238.

Findings—Between 4/2018–7/2019, 16 patients were screened for enrollment into the study. Of the 16 screened patients, two patients (12%) withdrew from the study and three (19%) were not eligible resulting in 11 patients (69%) who completed the trial. Intravenous administration of panitumumab-IRDye800CW at the dose of 25 mg, 50 mg, and 75 mg did not result in any grade 3 or higher AEs in PDAC patients. There were no serious AEs attributed to panitumumab-IRDye800CW, although four possibly related AEs (grade 1 and 2) were reported in four patients. The optimal dose based on TBR was identified as 50 mg (mean TBR 4·0). Intraoperatively, NIR fluorescence imaging provided enhanced visualization of the primary tumors, metastatic lymph nodes, and even small (2 mm) peritoneal metastasis.

Interpretation—To our knowledge, this study presents the first clinical use of panitumumab-IRDye800CW for detecting PDACs and shows that panitumumab-IRDye800CW is safe and feasible to use during pancreatic cancer surgery. Tumor-specific intraoperative imaging may have added value for treatment of patients with PDACs through improved patient selection and enhanced visualization of surgical margins, metastatic lymph nodes, and distant metastasis.

INTRODUCTION

Pancreatic ductal adenocarcinoma (PDAC) is predicted to be the second most common cause of cancer death by 2030[1], with a five-year survival rate of 9%[2]. Although complete surgical resection is the only curative option for these patients[3], little new technologies have been introduced over the past several decades to enhance the curability of surgery. Current preoperative cross-sectional imaging modalities, including computed tomography (CT), magnetic resonance imaging (MRI), and positron emission tomography (PET), lack sufficient resolution to detect small lesions, and therefore up to 25% of patients can be found to have radiologically occult metastatic lesions during laparoscopy or laparotomy [4,5]. In the operating room, surgeons cannot reliably distinguish the true extent of the primary tumor through visual inspection and palpation, owing to the peritumoral fibrotic stromal reaction and infiltrative patterns of pancreatic cancers. Intraoperative frozen section analysis has been used to assist surgeons to identify positive margins and metastatic lesions, however, it can suffer from sampling errors. Consequently, up to 85% of patients will develop recurrence even after surgery[6,7], due to tumor-positive margins[8] or metastasis unrecognized at the time of surgery[9]. Real-time identification of disease remains a critically unmet need to improve

intraoperative cancer detection and achieve a complete resection of the cancer, or if necessary abort a non-curative surgery.

Over the past decade, near-infrared (NIR) fluorescence-guide surgery has emerged as a promising technique for hepato-pancreato-biliary cancers using either non-specific fluorescent dyes (indocyanine green)[10–12] or tumor-specific fluorescent agents[13–16]. An ideal molecular fluorescence imaging agent should be safe to use, and be able to enhance visualization of primary tumors, detect tumor-positive margins, stage local-regional lymph nodes, and identify distant metastasis. We propose that fluorescent labeling of a therapeutic antibody with a NIR fluorophore for tumor-specific molecular imaging can leverage the known safety profile and binding specificity of the antibody to improve the translational safety and reduce time and costs[17–20] of introduction to patients. The epidermal growth factor receptor (EGFR) is a cell-surface marker that has been shown to be a suitable imaging target for pancreatic cancers based on its overexpression in both primary and metastatic PDACs[21,22]. Overexpression of EGFR has been reported in 64–95% of patients with PDAC[23–25]. In fact, our pilot study in four PDAC patients demonstrated the feasibility of using an anti-EGFR antibody - cetuximab to detect PDACs during surgery[15,16]. Our experience with cetuximab (a chimeric human mouse antibody) showed a significant number of infusion reactions which was inconsistent with a successful imaging agent[26]. As a result, we have expanded the use of anti-EGFR antibodies for intraoperative molecular imaging using a fully humanized anti-EGFR antibody (panitumumab) which has an improved safety profile.

In this study, we aimed to determine the optimal dose, safety, and feasibility of using panitumumab-IRDye800CW for molecular fluorescence-guided surgery in subjects with pancreatic cancer undergoing surgical intervention.

METHODS

Study design and patients

We performed a single-center, phase I, open-label, first-in-human study evaluating the dose, safety, and feasibility of panitumumab-IRDye800CW following a dose escalation study design.

We enrolled patients aged older than 19 years with a life expectancy of more than 12 weeks, with Karnofsky performance status of at least 70% or ECOG/Zubrod level 1, hemoglobin   9 gm/dL, platelet count   100,000/mm3, magnesium, potassium and calcium levels above the lower limit of normal per our institutional normal lab values, and TSH < 13 micro International Units/mL, who had clinically suspicious or biopsy-confirmed PDAC and were scheduled for standard of care surgery with curative intent.

We excluded patients who received an investigational drug within 30 days prior to first dose of panitumumab-IRDye800CW, or had myocardial infarction (MI), cerebrovascular accident (CVA), uncontrolled congestive heart failure (CHF), or unstable angina within 6 months prior to enrollment. Additional exclusion criteria included history of infusion reactions to panitumumab or other monoclonal antibody therapies, pregnancy or breastfeeding, evidence

of QTc prolongation on pretreatment ECG (>440 ms in males or > 460 ms in females), receipt of Class IA or II antiarrhythmic agents, or lab values that in the opinion of the physician would prevent surgical resection.

The study was conducted in accordance with the ethical principles that have their origin in the Declaration of Helsinki and FDA's ICH-GCP guidelines and the laws and regulations of the United States. All participants provided written informed consent, and the protocol was approved by the Stanford University Administrative Panel on Human Subjects Research and the FDA (ClinicalTrials.gov Identifier: NCT03384238).

Procedures

Panitumumab-IRDye800CW was produced by incubating panitumumab (Vectibix; Amgen, Thousand Oaks, California, USA; 147 kDa) and IRDye800CW-NHS (LI-COR Biosciences Inc., Licoln, NE, USA; 1.1 kDa) for 2-hours at 20°C in the dark with a dye to protein ratio of 2.3:1. Quality control measurements included analysis of drug product in sterile vial for particulates, and integrity of the sterilizing filter. Sterile vials were transported to Stanford University under temperature-controlled conditions and vials were stored and dispensed by the Stanford University Medical Center Investigational Pharmacy.

The half-life of panitumumab-IRDye800CW is dose-dependent and has been estimated to be on average 24 hours for doses up to 1.0 mg/kg, following an initial dose of 100 mg of unlabeled panitumumab[26]. Our previous clinical studies have shown that a 50 mg fixed dose is optimal for imaging both primary tumors[27] and metastatic lymph nodes[28] in patients with head and neck cancer. Furthermore, we have also found that both fluorescence intensity and tumor-to-background ratio (TBR) remained consistent within 2–5 days after infusion of panitumumab-IRDye800CW[27], suggesting that 2–5 days between infusion and surgery is ideal for surgical imaging.

In the dose escalation study, participants were sequentially assigned to 25mg, 50mg or 75 mg of panitumumab-IRDye800CW. We did not utilize blinding or include a placebo treatment. To assess for potential infusion reactions to panitumumab, but not the study drug (panitumumab-IRDye800CW), all study participants received a loading dose of 100 mg of panitumumab prior to infusion of panitumumab-IRDye800CW. The study drug was administrated 2–5 days prior to surgery. First, panitumumab was intravenously administrated over 1 hour followed by a 15 min observation period. Thereafter panitumumab-IRDye800CW was intravenously administered over 1 hour also followed by 1 hour of monitoring. Subjects who experienced a serious reaction to the test dose of unlabeled panitumumab did not proceed to receive panitumumab-IRDye800CW, and were not counted towards the study accrual target.

On the day of surgery, intraoperative NIR fluorescence imaging was performed at four instances during the course of the operation: directly after incision or laparoscopic access to the abdomen, after the tumor was exposed, when lymph nodes were encountered and after completion of resection (i.e. resection bed imaging). Diagnostic laparoscopy was performed selectively on patients with elevated CA19–9 (>150 U/mL) and large tumor size (> 3 cm). For open-field NIR fluorescence imaging, the IRDye800CW-tailored SPY-PHI imaging

platform (Novadaq, Burnaby, Canada), and the Explorer Air (SurgVision GmbH, Munich, Germany) were used. For laparoscopic fluorescence imaging the PINPOINT imaging platform (Novadaq, Burnaby, Canada) was used. Immediately following resection, tissue specimens, including margin samples, were imaged ex vivo in the closed-field NIR imaging devices, including IGP-ELVIS (margins, lymph node specimens) and PEARL Triology (primary tumor specimens) (LI-COR Biosciences Inc.) to allow for imaging in a controlled environment[29,30]. Upon completion of intraoperative imaging, tissue specimens were transported to pathology, fixed overnight in formalin, and grossed according to the standard of care (More details can be found in appendix p1). Formalin-fixed tissue samples were subsequently imaged in a closed-field NIR imaging device (Pearl Triology; LI-COR Biosciences Inc.), and paraffin-embedded after which 5 μm thick sections were obtained and stained for hematoxylin and eosin (H&E).

H&E slides were microscopically evaluated by a board-certified study pathologist (B.A.M.), who was blinded to the NIR fluorescence imaging data, and areas of tumor on the slides were outlined. For the relevant margins, including the pancreatic neck, bile duct, uncinate (retroperitoneal/superior mesenteric artery), proximal (gastric or duodenal) and distal (duodenal or jejunal) margin, the margin distance (i.e. tumor edge to specimen edge distance) was measured on the slides. Immunohistochemistry (IHC) was performed using an autostainer (DAKO Link48 with PT link; Agilent Technologies Inc., Santa Clara, CA, USA) to assess expression of the imaging target - EGFR (clone EP38Y; ThermoFisher Scientific, Waltham, MA, USA) in patient tissue.

To determine the optimal dose, fluorescence intensities of five regions of interest (ROI) were selected from the gross pancreatic tumor area and five ROIs were selected from the surrounding non-tumorous pancreas area from each SPY-PHI image of primary tumor in vivo using ImageJ.[31] ROIs were equally spaced and spread across each area whenever possible in the surgical field. The mean fluorescence intensity (MFI) of five tumor ROIs were averaged to represent the fluorescence signal of the primary tumor, and the MFI of five normal ROIs were averaged to represent the fluorescence signal of the non-tumor tissue. Here, the MFI of each ROI was defined as total fluorescence signal/ROI area, and the TBR for each tissue area was defined as the fluorescence signal of the tumor/fluorescence signal of the surrounding normal tissue.

To determine the sensitivity and specificity of using fluorescence to differentiate primary tumor from normal tissue, receiver operating characteristic (ROC) analysis was performed using the MFI of the formalin-fixed tissue in cassettes as a continuous measure. To distinguish metastatic lymph nodes from benign lymph nodes ex vivo, a logistic regression model was built with the covariants MFI and signal-to-background ratio (SBR) of each lymph node, as well as the random effect associated with each patient. A total of 384 lymph nodes were included in this analysis. Here, the SBR was calculated by dividing lymph node MFI by the adipose tissue MFI[28] as measured with Image Studio software (LI-COR Biosciences Inc.). In all the analysis of ex vivo tissue, pathology diagnosis was used as the gold standard for tumor detection. The optimal cut-off point or threshold was determined by the maximum value of the Youden index for each ROC curve. Subsequently, the sensitivity

(true positives / (true positive + false negatives) and specificity (true negatives / (true negative + false positives) were determined.

To assess the localization of panitumumab-IRDye800CW in the tissue, fluorescence microscopy was performed on selected tissue slides using a previously developed protocol[32]. Briefly, following deparaffinization, tissue slides were counterstained with 4', 6-diamidino-2-phenylindole (DAPI, Prolong Diamond, Thermo Fisher Scientific), coverslipped and dried overnight in the dark at room temperature. Slides were subsequently imaged on a custom-build inverted digital fluorescence microscope (DM6B, Leica Biosystems, Wetzlar, Germany) equipped with a highly sensitive Leica DFC9000GT camera (4.2M Pixel sCMOS camera), a metal halide LED light source (X-Cite 200DC, Excelitas Technologies, Waltham, Massachusetts, USA) for DAPI imaging, and a xenon arc lamp LB-LS/30 (Sutter Instrument, Novato, California, USA) for NIR microscopic imaging of panitumumab-IRDye800CW. Image acquisition and processing was done through LAS X software (Leica Biosystems).

Adverse events (AE) were reported based on federal regulations[33] and the National Cancer Institute Common Terminology Criteria for Adverse Events (v5.0). The severity of AEs were graded using the following criteria: (1) Mild (Grade 1); (2) Moderate (Grade 2); (3) Severe (Grade 3); (4) Immediately life-threatening/Fatal (Grade 4 and 5). The causality of adverse events were assessed using the following criteria: (1) Unrelated: There is no temporal relationship between the event and the administration of the study drug, and/or the event is clearly due to the subject's medical condition, other therapies, or accident. (2) Possibly Related: There is some temporal relationship between the event and the administration of the study drug and the event is unlikely to be explained by the participant's medical condition or other therapies. (3) Probably Related: The temporal relationship between the event and the administration of the study drug is compelling, and the participant's medical condition or other therapies cannot explain the event. (4) Definitely Related: The temporal relationship between the event and the administration of the study drug is compelling, the participant's medical condition or other therapies cannot explain the event and the event follows a known or suspected response pattern to the medication. Safety data and adverse events were collected at the day of infusion, day of surgery (2–5 days post-infusion of the study drug), and in follow up at day 15 (±4) and day 30 (±7). Physical exam, vital signs and Karnofsky performance status were assessed at screening, on the day of infusion (prior to and after study drug infusions), and in follow-up at day 15 (±4) and day 30 (±7). To assess QT/QTc interval changes, ECGs were obtained at screening, 30 min post-initiation of the loading dose of panitumumab, and 1 hour (±10 min) after completion of panitumumab-IRDye800CW infusion, and in follow-up on day 30 (±7). A previous ECG that was obtained as part of standard of care could be used as the screening ECG as long as it was obtained within 30 days of infusion of the study drugs. Patients were off-study after their day 30 (±7) follow-up.

Outcomes

The primary outcome of this study was to determine the optimal dose of panitumumab-IRDye800CW in identifying pancreatic cancer compared to surrounding normal tissue as

measured by TBR. TBR is defined as the MFI of tumor tissue divided by the MFI of surrounding pancreatic tissue.

The secondary outcomes of this study were safety and feasibility of using pantiumumab-IRDye800 for surgical-guidance in PDAC patients. The safety and tolerability of panitumumab-IRDye800CW were assessed by the number of grade 2 or higher adverse events that were determined to be clinically significant and definitely, probably or possibly related to panitumumab-IRDye800CW. Feasibility was determined by assessing whether metastatic lesions, tumor-positive lymph nodes and/or residual disease at resection margins could be detected by NIR fluorescence imaging of panitumumab-IRDye800CW in vivo and ex vivo.

Statistical analysis

Due to the exploratory nature of this study, we did not perform power calculation for sample size. Descriptive statistics, including the MFI and TBR were represented as mean and standard deviation (SD). The MFI of PDAC and surrounding uninvolved pancreas were compared using the two-tailed Mann-Whitney test. The MFI and SBR of the metastatic and benign lymph nodes were compared with the Mann-Whitney test as well. A P value of smaller than 0.05 was considered as statistically significant. The primary outcome (TBR per dosing cohort) was assessed in all patients with pathologically confirmed diagnosis of conventional PDAC. The secondary outcomes (safety and feasibility) were assessed in all the enrolled patients. Descriptive statistics and figures were generated using GraphPad Prism (Version 8.0, GraphPad Software, La Jolla, California, USA).

This study is registered with ClinicalTrials.gov, number NCT03384238.

Role of the funding sources

The report presents the results of an investigator-initiated study. The funding sources had no role in study design, data collection, analysis, and interpretation, or writing of this report. The corresponding author had full access to all the study data and the final responsibility to submit for publication.

RESULTS

Between 4/2018 and 7/2019, 16 patients were screened for enrollment into this phase I study. Of the 16 consented patients, two patients (12%) withdrew from the study before eligibility screening and three (19%) patients were not eligible, resulting in 11 patients (69%) completing the study (see appendix p2). The average age of the enrolled patients was 65 years (Table 1) and all patients were clinically diagnosed with PDAC. The study drug was administered 2–5 days prior to surgery, and the mean time from infusion to surgery was 58 hours. All patients received an intravenous infusion of unlabeled panitumumab as a loading dose (100 mg), followed by 25 mg (n=4), 50 mg (n=4), and 75 mg (n=3). Eight (73%) out of the 11 patients underwent a Whipple procedure to remove the tumor located in the pancreatic head. Two patients (18%) had pancreatic tail tumors and underwent laparoscopic distal pancreatectomy and splenectomy. One patient (9%) had both peritoneal and liver metastasis resulting in abortion of the surgical resection. On final pathology,

conventional PDAC was confirmed in nine (90%) of the 10 patients that underwent curative resection. The remaining single patient (10%) was diagnosed with a rare variant adenocarcinoma (mucinous/colloid carcinoma) and was included for safety analysis but excluded from further analysis. The reason for exclusion from fluorescence analysis is that the amount of neoplastic epithelium associated with the mucin was unusually sparse, requiring pathology review by experts at two major academic institutions to confirm the diagnosis. Although this rare subtype could represent a potential limitation of a visualization strategy targeting EGFR expression on cancer cells, inclusion of this particularly nonrepresentative case in our small cohort of patients would greatly skew the data and limit the generalizability to conventional ductal adenocarcinoma.

No infusion reactions occurred following panitumumab-IRDye800CW infusion, nor were any changes in blood chemistry levels observed. Although no AEs could be directly attributed to the study drug, a total of four AEs were reported that were considered "possibly related to the study" (Table 2). In one patient from Cohort 1, hypertension was reported (grade 2 AE). In Cohort 2, in one patient post-surgical presyncope was reported (grade 1 AE), and for another patient ECG changes (slightly prolonged QTc after infusion) were reported (grade 1 AE). In Cohort 3, vomiting (grade 1AE) was reported in one patient. There were no patients who discontinued for drug-related toxicity and no treatment-related deaths.

Intraoperative in vivo imaging demonstrated an enhanced fluorescence signal in the tumor compared to surrounding uninvolved pancreas in all three dosing cohorts (Fig. 1A). A relatively high background signal was observed in the liver (Fig. 1A, bottom right), because panitumumab-IRDye800, similarly to panitumumab, is cleared by the liver. As dose increased from 25 mg to 75 mg, the MFI of both the tumor and the background increased (see appendix p3). The TBR of primary tumors (as delineated by the surgeon intraoperatively) in the dosing cohorts of 25 mg, 50 mg, and 75 mg was $3 \cdot 0 \pm 0 \cdot 5$, $4 \cdot 0 \pm 0 \cdot 6$, and $3 \cdot 7 \pm 0 \cdot 4$, respectively (Fig. 1B). Enhanced fluorescence visualization was observed during open surgical procedures, but also during laparoscopic procedures where the surgeon had no tactile feedback (Fig. 2A). Macroscopic fluorescence imaging was correlated with histopathology by the study pathologist (Fig. 2B). The MFI of the histologically confirmed PDAC was significantly higher than that of surrounding uninvolved pancreas ex vivo (see appendix p4). Receiver operating characteristic (ROC) analysis (see appendix p4) showed that fluorescence can differentiate tumor from normal pancreas (ex vivo) with an area under the curve (AUC) of $0 \cdot 87$ (95% CI: $0 \cdot 83$–$0 \cdot 92$), a sensitivity of $90 \cdot 3\%$ (95% CI: $84 \cdot 5\%$ $-94 \cdot 2\%$), and a specificity of $74 \cdot 5\%$ (95% CI: $65 \cdot 1\%$$-82 \cdot 1\%$).

Intraoperative frozen section analysis of margins was performed in seven patients (pancreatic neck margin and/or bile duct margin) and were all diagnosed as negative for dysplasia or adenocarcinoma. For two patients whose tumors were located at the pancreatic body or tail, no margins were sent for frozen analysis and the proximal pancreatic parenchymal margins were evaluated by permanent pathology and diagnosed as uninvolved by invasive carcinoma and pancreatic high-grade intraepithelial neoplasia. For eight patients whose tumors were not located at the pancreatic body or tail, five surgical margins, including the pancreatic neck margin, bile duct margin, uncinate (retroperitoneal/superior mesenteric artery) margin, proximal margin (gastric or duodenal), and distal margin

(duodenal or jejunal) were assessed at pathology. The uncinate margins from 3 of these patients were read as involved by invasive carcinoma (tumor cells present within 1 mm distance to the uncinate margin). This correlated with fluorescence imaging (Fig. 3A): the fluorescence intensity dropped 3.5-times within 1 mm in patients with a tumor-positive margin, while the fluorescence remained unchanged in the tumor-negative margin (see appendix p5), suggesting that the variation of fluorescence signal within 1 mm distance to permanent margins could differentiate tumor-positive from tumor-negative surgical margin.

Intraoperatively, a total of 26 suspicious lymph nodes were individually harvested by the surgeon (in addition to the nodes harvested en bloc with the pancreatectomy specimen). Three of these nodes were found to contain metastatic adenocarcinoma (Fig. 4A–B). Intraoperative closed-field imaging of the fresh lymph nodes showed higher fluorescence signal in metastatic lymph nodes compared to benign lymph nodes (see appendix p6). After resection, these lymph nodes were formalin fixed and re-imaged prior to histopathological processing (Fig. 4C). In addition to the 26 individual lymph nodes harvested by the surgeon, another 358 lymph nodes were harvested from the submitted pancreatectomy specimens by the pathologist. Sixty-seven (17%) of the total of 384 lymph nodes were diagnosed as involved by metastatic adenocarcinoma. Both the MFI and the SBR of the metastatic lymph nodes were significantly higher than these of the benign lymph nodes (see appendix p6). The ROC curve (see appendix p6) using both MFI and SBR achieved an AUC value of 0·87 (95% CI: 0·83–0·91), a sensitivity of 67·2% (95% CI: 57·8%−80·6%), and a specificity of 92·1% (95% CI: 89·3%−94·4%).

Next we evaluated the effect of the dose of panitumumab-IRDye800CW on lymph node detection. Ranking the fluorescence intensity of individual lymph nodes in each patient (see appendix p7) showed the distribution of the true-positive, true-negative, false-positive, and false-negative lymph nodes. The 50 mg cohort showed the highest AUC value of 0·88 (95% CI: 0·77–0·95), with a sensitivity of 80·0% (95% CI: 57·1%−93·8%), and a specificity of 91·0% (95% CI: 84·5%−95·3%) (see appendix p7). Of the 52 fluorescent lymph nodes that did not contain tumor (false-positives), 31 (60%) were found in the 25 mg cohort, 9 (17%) were found in the 50 mg cohort, and 12 (23%) were found in the 75 mg cohort.

In one (9%) of the eleven patients surgery was aborted due to identification of distant metastasis. In this patient, a small peritoneal metastasis (< 2 mm), which cannot be readily identified both preoperatively and intraoperatively, especially during minimally invasive surgery, showed enhanced fluorescence in vivo (Fig. 5A). A suspicious liver lesion was also noted in this patient both under white light and fluorescence visualization (Fig. 5B). The suspected areas were biopsied for frozen section analysis and confirmed as metastatic adenocarcinoma consistent with pancreatic origin.

To verify that panitumumab is targeting EGFR in PDAC tissue, microscopic imaging of representative tissue regions was performed and demonstrated specific binding of panitumumab-IRDye800CW to PDACs in primary tumor, lymph node metastasis, perineural invasion, positive tumor margin, pancreatic intraepithelial neoplasia (panIN1–3), and pancreatitis (see appendix p8).

DISCUSSION

This first-in-human study demonstrated that intravenous administration of panitumumab-IRDye800CW at 50 mg provides the best tumor visualization in patients with PDAC among the three dosing cohorts, and that panitumumab-IRDye800CW is safe and feasible to evaluate surgical margins, metastatic lymph nodes, and distant metastasis. Intravenous administration of panitumumab-IRDye800CW at the dose of 25 mg, 50 mg, and 75 mg did not result in any grade 3 or higher AEs in PDAC patients. This study showed that panitumumab-IRDye800CW not only enhanced intraoperative visualization of disease during surgery, but more importantly, it provided additional information when the surgeon's ability to detect disease was limited during laparoscopic surgery. As minimally invasive surgical procedures, including laparoscopic and robotic pancreatic procedures continue to gain popularity, NIR fluorescence imaging using tumor-specific agents could provide an enhanced layer of information and help substitute for the lack of tactile information[34].

Our clinical trial experience in surgical imaging using fluorescence has focused on identification of the optimal dosing for surgical imaging based on two key elements - sufficient contrast between tumor and normal tissue (TBR) as well as a strong enough fluorescence signal to enhance tumor visualization (MFI). Since this study is an early phase clinical trial, the statistical considerations are limited. Multiple comparisons test for the three dosing groups did not identify a highest TBR with statistical significance. Our previous study showed that 50 mg is the optimal dose for imaging of both primary tumor[27] and metastatic lymph nodes[28] in patients with head and neck cancers. Based on our prior experience and current data, we selected 50 mg as the optimal dose, which provided the highest TBR among three dosing groups and a higher MFI than the cohort receiving 25 mg. These findings remain to be validated in a larger population in future studies. Importantly, this study demonstrated the feasibility of detecting small (< 2mm) peritoneal metastasis using panitumumab-IRDye800CW. Since conventional preoperative cross-sectional and functional imaging cannot reliably identify subradiologic disease, the surgical procedure often begins laparoscopically. The value of conventional preoperative imaging is further reduced in patients that receive neoadjuvant treatment. Discriminating viable tumor from chemotherapy or radiation-induced tumor necrosis and fibrosis becomes very challenging using conventional imaging strategies. This study suggests that intraoperative, tumor-specific fluorescence imaging can be used to survey the peritoneal cavity as well as the primary tumor locoregionally to potentially improve patient selection for curative surgery.

Moreover, this study also suggested that intraoperative back-table fluorescence imaging can be used to examine surgical margins and suspicious lymph nodes in the operating theater, which may provide efficient and important assessment of margins intraoperatively, which is crucial in pancreatic cancer surgery. However, it should be noted that the pancreatic neck margin is the only margin towards which resection can be extended intraoperatively in a meaningful and safe fashion. A positive margin in the uncinate process, retroperitoneum, and vascular groove can be an intraoperative challenge. Given that all frozen section margins were negative in our study, the role of this modality in margin assessment and enhancement remains to be determined. Furthermore, even if negative resection margin are achieved, median survival rates still remain suboptimal[35], suggesting the presence of occult disease

that is not detected and addressed during resection. Visually occult lymph node and distant metastases are thought to account for rapid recurrence of disease[8,9], leading to poor survival outcomes. Based on the high sensitivity and specificity of fluorescence imaging to identify occult metastatic lymph nodes, intraoperative molecular fluorescence imaging may help the surgeon identify metastatic lymph nodes in the resection bed after surgery for PDAC and proceed with their removal. Although we have previously observed high false-positive rate in the higher dose cohorts[16], here the high false-positive rate was found in the 25 mg cohort (see appendix p7), which was mainly driven by patient 1 who had a large number of fluorescent but pathologically negative lymph nodes. We have no biologically plausible explanation for this observation in the low-dose cohort.

This study also identified several challenges in the clinical translation of tumor-specific imaging tracers for pancreatic cancer. First, EGFR overexpression was found in pancreatitis that may have false-positive fluorescence uptake and confound cancer detection, which is consistent with our previous finding in a pilot study using cetuximab-IRDye800CW[15]. However, the level of fluorescence in pancreatitis has been shown to be significantly different from normal pancreas and pancreatic cancer[15], which suggests the feasibility of using a tumor-specific fluorescence agent to identify cancer. Second, although tumor-positive margins were clearly identified on surgical specimen using fluorescence imaging, we were unable to assess the value of fluorescence imaging in the surgical margins that were sent separately for frozen margins assessment since they were all negative. Next, only one patient was found with distant metastasis and it remains unclear in how many of the other patients metastases were missed, so the value of this technique for identifying distant metastasis needs to be further examined in future studies. Finally, it remains unclear how preoperative treatment with chemotherapy and/or radiotherapy could affect fluorescence imaging of pancreatic cancer. Changes in the size or viability after pretreatment may affect the sensitivity of intraoperative cancer imaging. A previous study[11] using a non-specific fluorescent agent (indocyanine green) during pancreatic cancer surgery reported correlation of fluorescence and response to neoadjuvant therapy in four patients. Using a tumor-specific agent in our study, we have observed enhanced visualization of tumors during surgery in all the patients irrespective of whether they received prior chemotherapy or radiation therapy (these patients presented with viable residual cancer cells on final pathology). Since our study was not designed or powered to analyze this problem, future investigation in a larger cohort of patients will be needed to further elucidate the fidelity of the molecular imaging agents in the setting of neoadjuvant therapy.

In summary, this first-in-human, dose-escalation study showed that panitumumab-IRDye800CW is safe and feasible to use for fluorescence-guided surgery in patients with pancreatic cancer undergoing surgical intervention, and has the potential to improve patient selection and enhance visualization of surgical margins, metastatic lymph nodes, and distant metastasis. The safety, dose, and surgical timing associated with the use of panitumumab-IRDye800CW in this study can be used to inform future studies. To determine the clinical value of this intraoperative imaging modality in a larger cohort of pancreatic cancer patients, a phase 2 study is planned to assess its incremental benefit over white light standard imaging in visualizing tumor margins, nodal and distant metastases in a statistically important manner.

Supplementary Material

Refer to Web version on PubMed Central for supplementary material.

REFERENCES

1. Rahib L, Smith BD, Aizenberg R, Rosenzweig AB, Fleshman JM, Matrisian LM. Projecting Cancer Incidence and Deaths to 2030: The Unexpected Burden of Thyroid, Liver, and Pancreas Cancers in the United States. Cancer Research 2014; 74(11): 2913–21. [PubMed: 24840647]

2. Siegel RL, Miller KD, Jemal A. Cancer statistics, 2019. CA: A Cancer Journal for Clinicians 2019; 69(1): 7–34. [PubMed: 30620402]

3. Hartwig W, Hackert T, Hinz U, et al. Pancreatic cancer surgery in the new millennium: better prediction of outcome. Ann Surg 2011; 254(2): 311–9. [PubMed: 21606835]

4. Maithel SK, Maloney S, Winston C, et al. Preoperative CA 19–9 and the yield of staging laparoscopy in patients with radiographically resectable pancreatic adenocarcinoma. Ann Surg Oncol 2008; 15(12): 3512–20. [PubMed: 18781364]

5. De Rosa A, Cameron IC, Gomez D. Indications for staging laparoscopy in pancreatic cancer. HPB : the official journal of the International Hepato Pancreato Biliary Association 2016; 18(1): 13–20. [PubMed: 26776846]

6. Lee J-c, Ahn S, Cho IK, Lee J, Kim J, Hwang J-H. Management of recurrent pancreatic cancer after surgical resection: a protocol for systematic review, evidence mapping and meta-analysis. BMJ Open 2018; 8(4): e017249.

7. Schnelldorfer T, Ware AL, Sarr MG, et al. Long-Term Survival After Pancreatoduodenectomy for Pancreatic Adenocarcinoma: Is Cure Possible? Annals of Surgery 2008; 247(3): 456–62. [PubMed: 18376190]

8. Tummers WS, Groen JV, Sibinga Mulder BG, et al. Impact of resection margin status on recurrence and survival in pancreatic cancer surgery. BJS 2019; 106(8): 1055–65.

9. Hishinuma S, Ogata Y, Tomikawa M, Ozawa I, Hirabayashi K, Igarashi S. Patterns of recurrence after curative resection of pancreatic cancer, based on autopsy findings. Journal of Gastrointestinal Surgery 2006; 10(4): 511–8. [PubMed: 16627216]

10. Ishizawa T, Fukushima N, Shibahara J, et al. Real-time identification of liver cancers by using indocyanine green fluorescent imaging. Cancer 2009; 115(11): 2491–504. [PubMed: 19326450]

11. Newton AD, Predina JD, Shin MH, et al. Intraoperative Near-infrared Imaging Can Identify Neoplasms and Aid in Real-time Margin Assessment During Pancreatic Resection. Annals of Surgery 2019; 270(1): 12–20. [PubMed: 31188797]

12. van der Vorst JR, Schaafsma BE, Hutteman M, et al. Near-infrared fluorescence-guided resection of colorectal liver metastases. Cancer 2013; 119(18): 3411–8. [PubMed: 23794086]

13. Hoogstins CES, Boogerd LSF, Sibinga Mulder BG, et al. Image-Guided Surgery in Patients with Pancreatic Cancer: First Results of a Clinical Trial Using SGM-101, a Novel Carcinoembryonic Antigen-Targeting, Near-Infrared Fluorescent Agent. Annals of Surgical Oncology 2018; 25(11): 3350–7. [PubMed: 30051369]

14. Lwin TM, Hoffman RM, Bouvet M. The development of fluorescence guided surgery for pancreatic cancer: from bench to clinic. Expert Review of Anticancer Therapy 2018; 18(7): 651–62. [PubMed: 29768067]

15. Tummers WS, Miller SE, Teraphongphom NT, et al. Intraoperative Pancreatic Cancer Detection using Tumor-Specific Multimodality Molecular Imaging. Annals of Surgical Oncology 2018; 25(7): 1880–8. [PubMed: 29667116]

16. Tummers WS, Miller SE, Teraphongphom NT, et al. Detection of visually occult metastatic lymph nodes using molecularly targeted fluorescent imaging during surgical resection of pancreatic cancer. HPB : the official journal of the International Hepato Pancreato Biliary Association 2019; 21(7): 883–90. [PubMed: 30723062]

17. Rosenthal EL, Warram JM, de Boer E, et al. Safety and Tumor-specificity of Cetuximab-IRDye800 for Surgical Navigation in Head and Neck Cancer. Clinical Cancer Research 2015: clincanres.3284.2014.

18. Rosenthal E, Moore L, Tipirneni K, et al. Sensitivity and Specificity of Cetuximab-IRDye800CW to Identify Regional Metastatic Disease in Head and Neck Cancer. Clinical Cancer Research 2017: clincanres.2968.016.

19. Lamberts LE, Koch M, de Jong JS, et al. Tumor-Specific Uptake of Fluorescent Bevacizumab–IRDye800CW Microdosing in Patients with Primary Breast Cancer: A Phase I Feasibility Study. Clinical Cancer Research 2017; 23(11): 2730–41. [PubMed: 28119364]

20. Gao RW, Teraphongphom NT, van den Berg NS, et al. Determination of Tumor Margins with Surgical Specimen Mapping Using Near-Infrared Fluorescence. Cancer Research 2018; 78(17): 5144–54. [PubMed: 29967260]

21. Tummers WS, Farina-Sarasqueta A, Boonstra MC, et al. Selection of optimal molecular targets for tumor-specific imaging in pancreatic ductal adenocarcinoma. Oncotarget 2017; 8(34): 56816–28. [PubMed: 28915633]

22. de Geus SW, Boogerd LS, Swijnenburg RJ, et al. Selecting Tumor-Specific Molecular Targets in Pancreatic Adenocarcinoma: Paving the Way for Image-Guided Pancreatic Surgery. Molecular imaging and biology 2016; 18(6): 807–19. [PubMed: 27130234]

23. Bloomston M, Bhardwaj A, Ellison EC, Frankel WL. Epidermal Growth Factor Receptor Expression in Pancreatic Carcinoma Using Tissue Microarray Technique. Digestive Surgery 2006; 23(1–2): 74–9. [PubMed: 16717472]

24. Xiong HQ, Rosenberg A, LoBuglio A, et al. Cetuximab, a Monoclonal Antibody Targeting the Epidermal Growth Factor Receptor, in Combination With Gemcitabine for Advanced Pancreatic Cancer: A Multicenter Phase II Trial. Journal of Clinical Oncology 2004; 22(13): 2610–6. [PubMed: 15226328]

25. Park SJ, Gu MJ, Lee DS, Yun SS, Kim HJ, Choi JH. EGFR expression in pancreatic intraepithelial neoplasia and ductal adenocarcinoma. International journal of clinical and experimental pathology 2015; 8(7): 8298–304. [PubMed: 26339400]

26. Gao RW, Teraphongphom N, de Boer E, et al. Safety of panitumumab-IRDye800CW and cetuximab-IRDye800CW for fluorescence-guided surgical navigation in head and neck cancers. Theranostics 2018; 8(9): 2488–95. [PubMed: 29721094]

27. Nishio N, van den Berg NS, van Keulen S, et al. Optimal Dosing Strategy for Fluorescence-Guided Surgery with Panitumumab-IRDye800CW in Head and Neck Cancer. Molecular imaging and biology 2020; 22(1): 156–64. [PubMed: 31054001]

28. Nishio N, van den Berg NS, van Keulen S, et al. Optical molecular imaging can differentiate metastatic from benign lymph nodes in head and neck cancer. Nature Communications 2019; 10(1): 5044.

29. van Keulen S, van den Berg NS, Nishio N, et al. Rapid, non-invasive fluorescence margin assessment: Optical specimen mapping in oral squamous cell carcinoma. Oral Oncology 2019; 88: 58–65. [PubMed: 30616798]

30. van Keulen S, Nishio N, Birkeland A, et al. The Sentinel Margin: Intraoperative ex-vivo Specimen Mapping Using Relative Fluorescence Intensity. Clinical Cancer Research 2019: clincanres.0319.2019.

31. Schindelin J, Arganda-Carreras I, Frise E, et al. Fiji: an open-source platform for biological-image analysis. Nature Methods 2012; 9(7): 676–82. [PubMed: 22743772]

32. Lu G, Fakurnejad S, Martin BA, et al. Predicting Therapeutic Antibody Delivery into Human Head and Neck Cancers. Clinical Cancer Research 2020: clincanres.3717.2019.

33. Gliklich RE, Dreyer NA, Leavy MB. Registries for evaluating patient outcomes: a user's guide. 3rd edition ed: Rockville (MD): Agency for Healthcare Research and Quality (US); 2014.

34. Gagner M, Palermo M. Laparoscopic Whipple procedure: review of the literature. Journal of hepato-biliary-pancreatic surgery 2009; 16(6): 726–30. [PubMed: 19636494]

35. Ghaneh P, Kleeff J, Halloran CM, et al. The Impact of Positive Resection Margins on Survival and Recurrence Following Resection and Adjuvant Chemotherapy for Pancreatic Ductal Adenocarcinoma. Ann Surg 2019; 269(3): 520–9. [PubMed: 29068800]

Research in context

Evidence before this study

Although surgical resection is the only curative option for pancreatic ductal adenocarcinoma (PDAC), up to 85% of resected patients will develop recurrence due to locoregional residual disease or metastasis unrecognized at the time of surgery. Tumor-specific fluorescent molecular imaging has the potential to enhance the surgeon's ability to detect the extent and location of pancreatic cancer in real-time in the operating room. We searched PubMed for publications using the terms "pancreatic cancer", "pancreatic ductal adenocarcinoma", "fluorescence-guided surgery", "intraoperative optical imaging" and "clinical trial", from database inception until March 7, 2020. We identified three clinical studies reporting on fluorescence-guided surgery in pancreatic cancers. Of these three clinical studies, only two used tumor-specific imaging agents. The first published study was our pilot study using cetuximab-IRDye800CW, a fluorescently labeled anti-epidermal growth factor receptor (EGFR) antibody. The second published study reported a phase I exploratory study using SGM-101, a fluorescently labeled anti-carcinoembryonic antigen (CEA) antibody.

EGFR is overexpressed in 64–95% of pancreatic cancers. In our current study, we demonstrate the benefit of EGFR based imaging, adding to our previous pilot study using cetuximab-IRDye800CW. We present evidence using a fully humanized antibody (panitumumab) labeled with IRDye800CW (panitumumab-IRDye800CW) as an imaging agent for PDAC because of its improved safety profile compared to cetuximab which is human-mouse chimeric.

Added value of this study

To our knowledge, this study describes the first clinical application of panitumumab-IRDye800CW in patients with PDAC for intraoperative detection of primary tumor and metastasis. This study demonstrates that intravenous administration of 25 to 75 mg of panitumumab-IRDye800CW is safe and tolerable in patients with PDAC, and that panitumumab-IRDye800CW is sensitive and specific for the detection of PDACs. Importantly, panitumumab-IRDye800CW allows for detection of occult lymph node metastasis and small peritoneal metastasis, which could improve lymph node staging and spare patients non-curative surgeries. This study also suggests that tumor-specific imaging may help surgeons identify tumor-positive margins.

Implications of all available evidence

Tumor-specific fluorescence imaging using panitumumab-IRDye800CW may provide surgeons enhanced visualization of positive surgical margins, metastatic lymph nodes, and radiographically occult peritoneal metastasis in patients with PDAC. To determine the clinical value of this intraoperative imaging modality in a larger patient cohort, a phase 2 study is planned to assess its benefit over white light standard imaging in visualizing tumor margins, nodal and distant metastases.
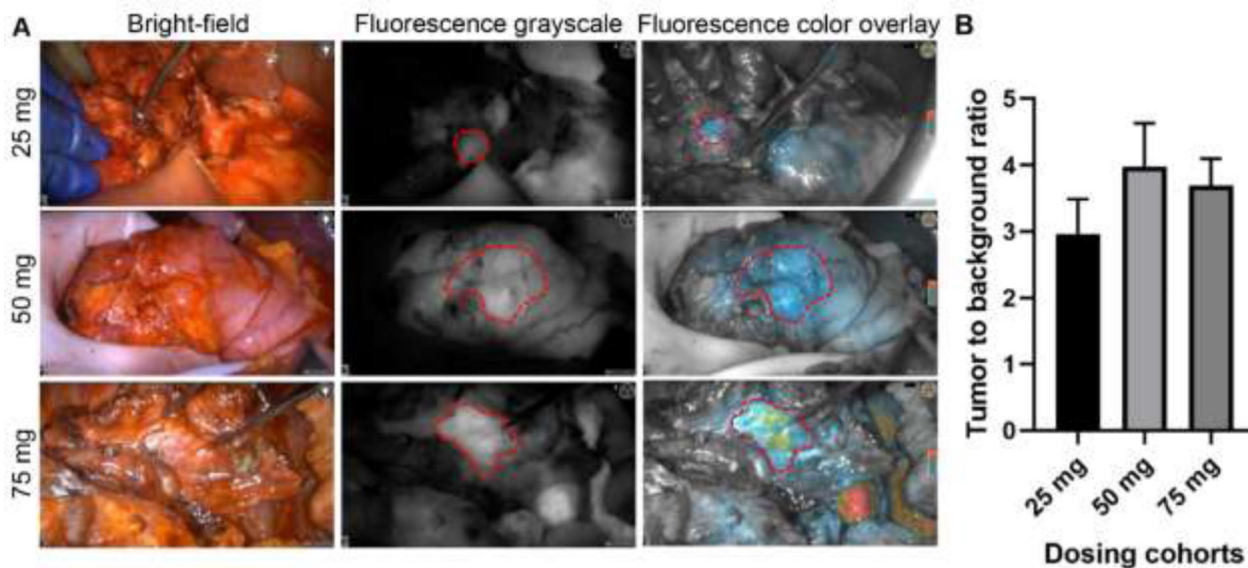
Figure 1.
Intraoperative fluorescence imaging showed enhanced visualization of primary tumors with varying doses. **A**. Representative bright-field, fluorescence grayscale, and fluorescence color overlay of patients infused at 25 mg, 50 mg, and 75 mg of panitumumab-IRDye800CW. Please note that the false-positive fluorescence uptake in the non-cancerous pancreas with pancreatitis (right panel, 25 mg) and in the liver in the bottom right corner of the 75 mg case **B**. Comparison of the in vivo TBR of patients undergoing open surgery showed that 50 mg provided the highest (but not statistically significant) TBR among the three dosing cohorts. The bar graphs plotted mean with standard deviation.
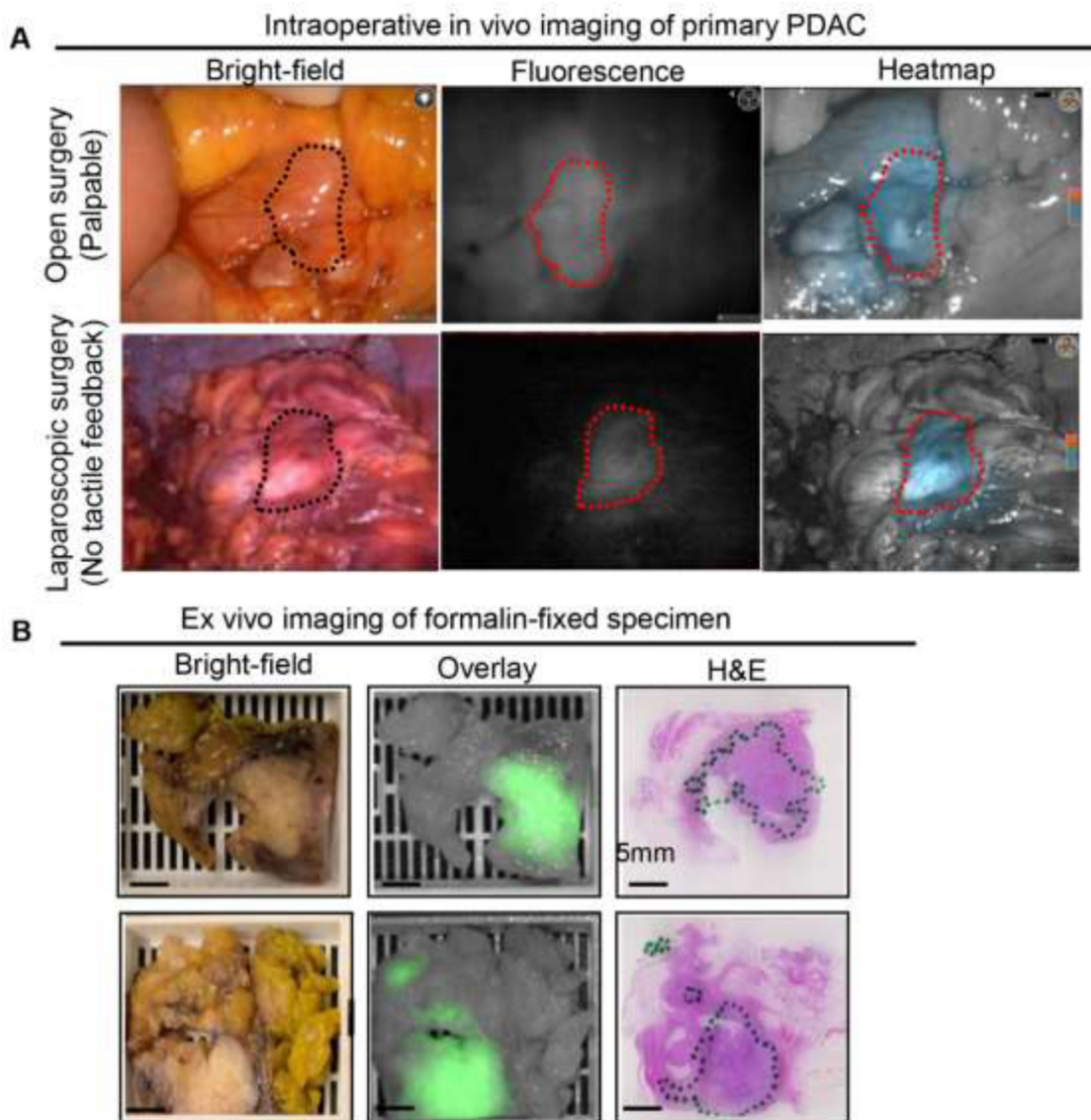
Figure 2.
Fluorescence imaging of primary PDAC showed good correlation with histopathology diagnosis. **A**. Intraoperative imaging showed enhanced visualization of primary tumors during both open surgery (Whipple) and laparoscopic surgery. **B**. Representative example images of formalin-fixed PDAC tissue in cassettes and corresponding H&E images (green outline means tumor region).
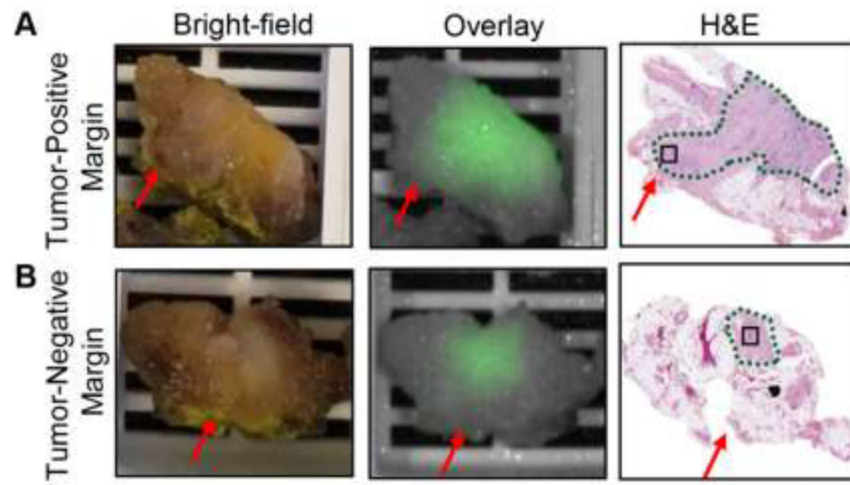
Figure 3.

Feasibility of using fluorescence imaging to detect tumor-positive margins. **A-B**. Representative images a tumor-positive margin and a tumor-negative margin.
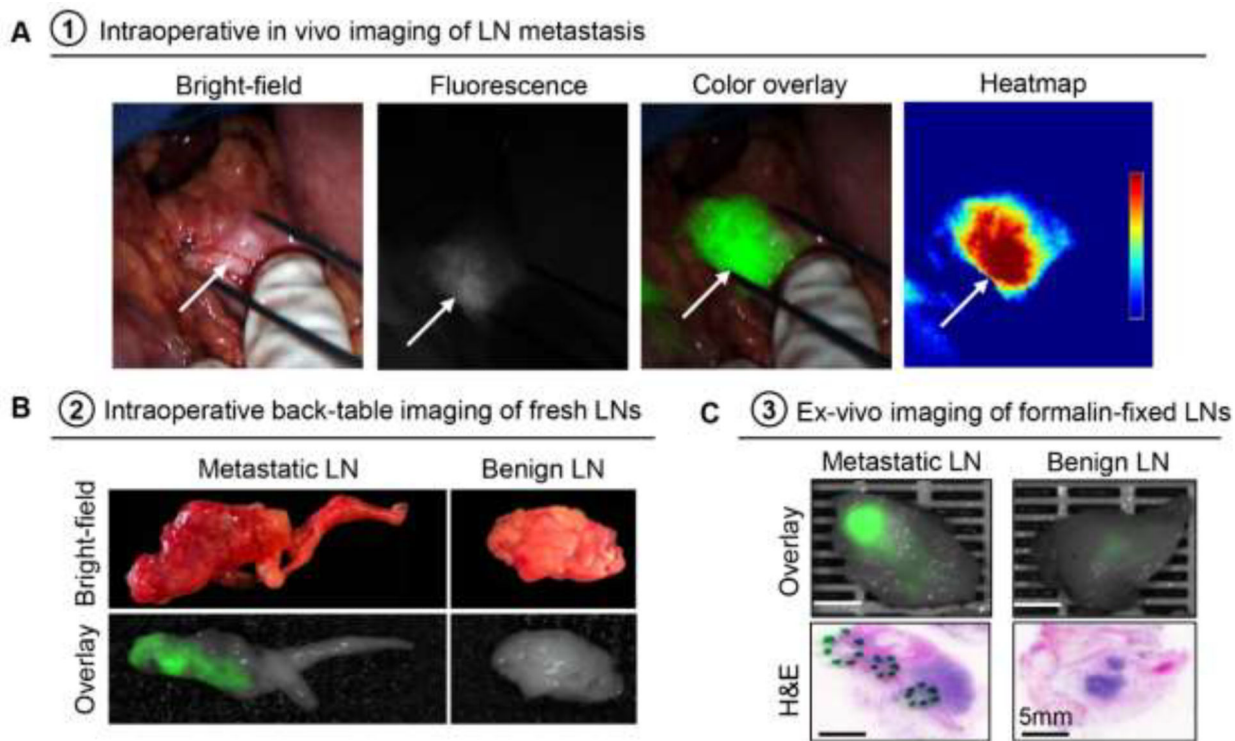
Figure 4.
Fluorescence imaging can identify metastatic lymph nodes intraoperatively in vivo and in the back-table in the operating room. **A**. In vivo fluorescence imaging of a tumor-positive lymph node. **B**. Back-table imaging of metastatic and benign lymph nodes (fresh tissue). **C**. Representative images of formalin-fixed metastatic and benign lymph nodes.
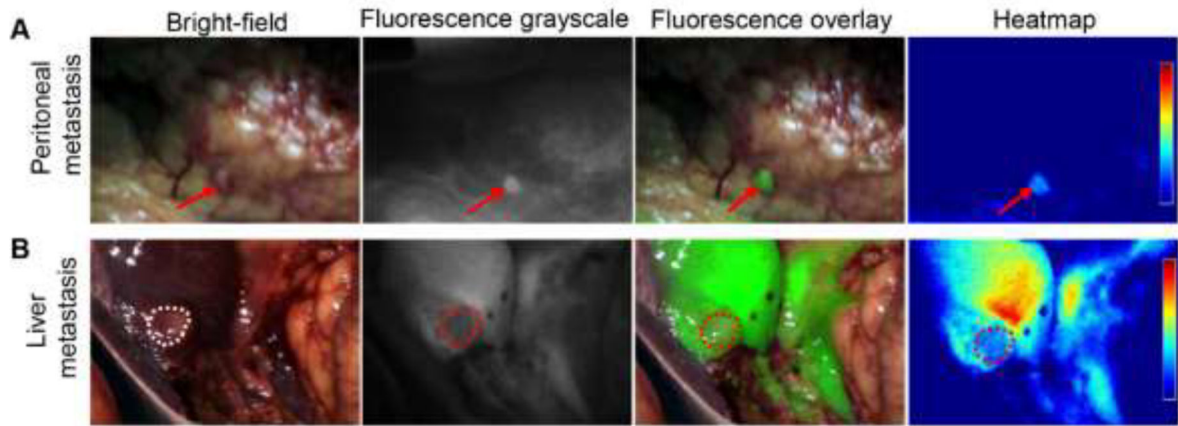
Figure 5.
Intraoperative fluorescence imaging can identify small distant metastatic lesions. **A**. Intraoperative imaging of a 2 mm peritoneal metastasis. **B**. Intraoperative imaging of a metastatic liver lesion demonstrates a negative fluorescence due to high intrinsic liver signal.

Table 1.

Patient demographics and clinical data

Study cohort	Patient	Age (years)	Surgical procedure	Tumor site	Histopathology Diagnosis	Pathology stage	Tumor size (cm)	Prior Chemo	Prior Radiation
Cohort 1 (25 mg)	1	68	Whipple	Pancreatic head	PDAC	T2N2Mx	2.1	No	No
	2	77	Whipple	Pancreatic head	PDAC	T2N0Mx	3	Four cycles FOLFIRINOX. Oxaliplatin and irinotecan reduced at cycle 4.	Yes
	3	59	Gastro-jejunostomy, Hepatico-jejunostomy	Panreatic head	PDAC	TxNxMl	N/A	No	No
	4	67	Whipple	Pancreatic head	PDAC (colloid carcinoma)	T3N1Mx	5	No	No
Cohort 2 (50 mg)	5	59	Whipple	Pancreatic head	PDAC	T3N2Mx	4.5	No	No
	6	59	Laparoscopic distal pancreatectomy	Pancreatic body and tail	PDAC	T3N1M1	5.2	No	No
	7	69	Whipple	Ampulla	Ampullary adenocarcinoma (pancreaticobiliary-type)	T3bN1Mx	3.1	No	No
		82	Laparoscopic distal pancreatectomy	Pancreatic tail	PDAC	T4N0Mx	3.6	Gemcitabine and Abraxane (3 cycles) and then single Gemcitabine	No
Cohort 3 (75 mg)	9	74	Whipple	Pancreatic head	PDAC	T2N2Mx	2.4	FOLFIRINOX (4 cycles)	No
	10	67	Whipple	Pancreatic head	PDAC	T2N1Mx	3.8	FOLFIRINOX (6 cycles)	No
	11	40	Whipple	Pancreatic head	PDAC	T3N2Mx	4.1	FOLFIRINOX (2 cycles) Irinotecan added for cycle 3–5	Yes

Table 2

Adverse events

Dosing cohort	Patient	Time	CTCAE Category	Toxicity	Serious adverse event	Severity	Relationship to Panitumumab-IRDye800CW
25 mg	1	Day 30	Gastrointestinal disorders	Constipation	No	Mild	Unrelated
			Investigations	Weight loss	No	Mild	Unrelated
	2	Day 16	Investigations	Weight loss	No	Mild	Unrelated
		Day 30	Gastrointestinal disorders	Nausea	No	Moderate	Unrelated
			General disorders and administration site conditions	Fatigue	No	Moderate	Unrelated
			Gastrointestinal disorders	Belching	No	Moderate	Unrelated
			Gastrointestinal disorders	Gastrointestinal disorders - Other, specify	No	Mild	Unrelated
			Gastrointestinal disorders	Abdominal pain	No	Mild	Unrelated
			Metabolism and nutrition disorders	Hypokalemia	No	Severe	Unrelated
	3	Day 1	Vascular disorders	Hypertension	No	Moderate	Possibly related
		Day 16	Gastrointestinal disorders	Abdominal pain	No	Mild	Unrelated
		Day 30	Gastrointestinal disorders	Belching	No	Mild	Unrelated
			Cardiac disorders	Atrial fibrillation	No	Moderate	Unrelated
			Gastrointestinal disorders	Abdominal pain	No	Moderate	Unrelated
			Gastrointestinal disorders	Nausea	No	Moderate	Unrelated
			Cardiac disorders	Sinus tachycardia	No	Mild	Unrelated
			Gastrointestinal disorders	Ileus	No	Moderate	Unrelated
	4	Day 16	Surgical and medical procedures	Surgical and medical procedures - Other, specify	No	Moderate	Unrelated
		Day 30	Gastrointestinal disorders	Gastrointestinal disorders - Other, specify	No	Mild	Unrelated
50 mg	5	Day 16	General disorders and administration site conditions	Fatigue	No	Mild	Unrelated
			Gastrointestinal disorders	Diarrhea	No	Mild	Unrelated
			Surgical and medical procedures	Surgical and medical procedures - Other, specify	No	Mild	Unrelated
	6	Day 30	General disorders and administration site conditions	Fatigue	No	Mild	Unrelated
			Musculoskeletal and connective tissue disorders	Musculoskeletal and connective tissue disorder - Other, specify	No	Mild	Unrelated
	7	Day 2	Nervous system disorders	Presyncope	No	Mild	Possibly related
	8	Day 1	Vascular disorders	Hypertension	No	Moderate	Unrelated
			Investigations	Electrocardiogram QT corrected interval prolonged	No	Mild	Possibly related
		Day 16	Gastrointestinal disorders	Abdominal pain	No	Mild	Unrelated
			Gastrointestinal disorders	Nausea	No	Moderate	Unrelated

Dosing cohort	Patient	Time	CTCAE Category	Toxicity	Serious adverse event	Severity	Relationship to Panitumumab-IRDye800CW
			Gastrointestinal disorders	Gastrointestinal disorders - Other, specify	No	Mild	Unrelated
		Day 30	Surgical and medical procedures	Surgical and medical procedures - Other, specify	No	Mild	Unrelated
75 mg	9	Day 16	Gastrointestinal disorders	Gastrointestinal disorders - Other, specify	No	Moderate	Unrelated
			General disorders and administration site conditions	Edema limbs	No	Mild	Unrelated
		Day 30	Vascular disorders	Hypertension	No	Moderate	Unrelated
			Gastrointestinal disorders	Diarrhea	No	Moderate	Unrelated
	10	Day 30	Investigations	Weight loss	No	Mild	Unrelated
	11	Day 1	Gastrointestinal disorders	Vomiting	No	Mild	Possibly related
		Day 16	Musculoskeletal and connective tissue disorders	Buttock pain	No	Mild	Unrelated